



Contents lists available at ScienceDirect

## Chemical Data Collections

journal homepage: [www.elsevier.com/locate/cdc](http://www.elsevier.com/locate/cdc)

## Data article

# Synthesis and antimicrobial activity evaluation of some new 7-substituted quinolin-8-ol derivatives: POM analyses, docking, and identification of antibacterial pharmacophore sites



Mohamed El Faydy<sup>a</sup>, Naoufal Dahaieh<sup>b</sup>, Khadija Ounine<sup>b</sup>, Vesna Rastija<sup>c</sup>,  
Faisal Almalki<sup>d</sup>, Joazaizulfazli Jamalis<sup>e</sup>, Abdelkader Zarrouk<sup>f</sup>,  
Taïbi Ben Hadda<sup>d,g,\*</sup>, Brahim Lakhri<sup>g</sup>

<sup>a</sup>Laboratory of Organic, Inorganic Chemistry, Electrochemistry, and Environment, Department of Chemistry, Faculty of Sciences, Ibn Tofail University, PO Box 133, 14000, Kenitra, Morocco

<sup>b</sup>Laboratory of Nutrition, Health, and Environment, Department of Biology, Faculty of Sciences, Ibn Tofail University, PO Box 133, 14000, Kenitra, Morocco

<sup>c</sup>Department of Agroecology, and Environmental Protection, Faculty of Agrobiotechnical Sciences Osijek, Josip Juraj Strossmayer University of Osijek, Osijek, Croatia

<sup>d</sup>Department of Pharmaceutical Chemistry, Faculty of Pharmacy, Umm Al-Qura University, Makkah Almukarramah, Saudi Arabia

<sup>e</sup>Department of Chemistry, Faculty of Sciences, University Teknologi Malaysia, 81310, Johor Bahru, Johor, Malaysia

<sup>f</sup>Laboratory of Materials, Nanotechnology, and Environment, Department of Chemistry, Faculty of Sciences, Mohammed V University, Avenue Ibn Battouta, PO Box 1014, Agdal-Rabat, Morocco

<sup>g</sup>Laboratory of Applied Chemistry, and Environment, Faculty of Sciences, Mohammed Premier University, MB 524, 60000 Oujda, Morocco

## ARTICLE INFO

## Article history:

Received 10 August 2020

Revised 3 November 2020

Accepted 8 November 2020

Available online 21 November 2020

## Keywords:

Synthesis

Quinolin-8-ol

Docking

POM (Petra/Osiris/Molinspiration analyses)

Antibacterial pharmacophore site

## ABSTRACT

Eight new 7-substituted quinolin-8-ol derivatives were synthesized in moderate to good yields through quinolin-8-ol, and secondary amines as the starting reagents. The structures of the prepared compounds have been characterized by elemental analysis and <sup>1</sup>H/<sup>13</sup>C NMR. The antimicrobial activity of this new series of heterocyclic compounds has been achieved "in vitro" against some bacterial strains by means of the disk method, and most of the tested compounds have shown comparable or greater antibacterial activity than nitroxoline (standard antibiotic). It was very motivating to observe that POM (Petra/Osiris/Molinspiration) bioinformatic analyses of compound **5** exhibited better antibacterial activity (MIC = 10 μg/mL against *B. subtilis* bacteria), and higher drug score (DS = 0.57) compared with Nitroxoline (DS = 0.47; MIC = 20 μg/mL). Molecular docking investigations were also conducted to investigate the binding affinities as well as interactions of some compounds with the target proteins.

© 2020 Elsevier B.V. All rights reserved.

\* Corresponding authors.

E-mail addresses: [taibi.ben.hadda@gmail.com](mailto:taibi.ben.hadda@gmail.com) (T.B. Hadda), [brahim.lakhri@uit.ac.ma](mailto:brahim.lakhri@uit.ac.ma) (B. Lakhri).

## Specifications Table

Subject area	Medicinal Chemistry.
Compounds	7-substituted quinolin-8-ol derivatives
Data category	Organic synthesis, Drug Design, Spectral, Computational analyses, Antibacterial activity.
Data acquisition format	<sup>1</sup> H NMR, <sup>13</sup> C NMR, IR, Elemental analysis.
Data type	Analyzed and simulated.
Procedure	Organic synthesis: Chemical reaction between 8-hydroxyquinoline and secondary amines. Analysis of antibacterial activity by using Molecular docking and bioinformatic POM Platform-2018.
Data accessibility	All data are included in this article

## 1. Rationale

Infectious and parasitic diseases are a major public health problem due to their frequency and severity [1]. The situation is more worrying because of the emergence of antibiotic-resistant microorganism strains, and the appearance of infrequent infections that compromise treatments with available drugs [2]. Faced with these numerous obstacles to the use of available antibacterials, it is important for researchers to find new effective antibacterial substances with a broad spectrum of action. The chemical synthesis of new molecules continues to the present day to produce new antibacterial that can contribute to combating antibiotic-resistant bacteria [3].

Quinoline is one of the most significant *N*-based heterocyclic aromatic molecules. Quinoline derivatives have recently attracted the attention of several researchers thanks to their broad fields of applications, and also for their vast scope of potential activities [4-6]. Heterocycles that include the quinoline scaffold possess a wide range of pharmacological activities [7,8]. Cloquinol is an antifungal, and antiprotozoal medicament [9]. It is also neurotoxic at high concentrations. A few 8-aminoquinoline compounds, for example, Primaquine, have been employed as chemotherapeutics for the treatment of malaria disease [10]. Hydroxyquinoline is a heterocyclic compound derivative of quinoline that has a two-ring system: phenol and pyridine rings. The quinolin-8-ol derivatives are frequently employed as chelating reagents in analytical chemistry, and radiochemistry for metal ion extraction and fluorometric determination [11,12]. In addition, quinolin-8-ol displays a pharmacophore associated with a variety of biological activities; these include inhibitors of HIV integrase [13], antibacterial [14], antifungal [15], and antitumor agents [16]. The modifications at the C-5, C-7, and C-8 position of the quinolin-8-ol was proved as an effective approach in drug design [17]. Thus, the introduction of a heterocyclic substituent at C-5 of quinolin-8-ol moiety might increase the biological potencies of these compounds [18].

The objective of the present work is to graft a piperazine moiety and other secondary aliphatic amines in C-7 of quinolin-8-ol by adopting the Mannich reaction. The incorporated compounds **1-8** (Fig. 1) were identified by <sup>1</sup>H, <sup>13</sup>C NMR, and elementary analysis. Their potential antibacterial effects against Gram-positive and Gram-negative microorganisms were screened. Filamenting temperature-sensitive mutant (FtsZ) is a prokaryotic homolog of eukaryotic cytoskeletal that serves as a scaffold during the bactericidal cell division. FtsZ contains four main protein domains: variable *N*-terminal enzymatic segment, core region, a variable spacer, and a C-terminal subdomain. *N*- and C-terminal subdomain are separated by a central core helix (H7 helix). A nucleotide-binding pocket is in the *N*-terminal subdomain (residues 12-171), while the C-terminal subdomain is a GTP-ase-activating subdomain (residues 223-310). In the presence of GTP, FtsZ polymerizes into tubulin-like protofilaments important for the formation, and constriction of the cytokinetic ring. [19-21]. The powerful inhibitor that targets FtsZ and inhibits bactericidal cell division of pathogens *Staphylococcus aureus* and *Bacillus subtilis* is the benzamide derivative PC19072.

The structure of the complex with the inhibitor PC190723 showed that the inhibitor binds at the cleft between the two subdomains, thereby promoting the polymerization of FtsZ reducing the GTPase activity [22]. In this study, the interactions of the 7-substituted quinolin-8-ol derivatives with the PC190723-binding site of SaFtsZ have been evaluated by molecular docking in order to confirm experimental results and to clarify the binding mode of inhibitor, and determine the structural features important for the antibacterial activity.

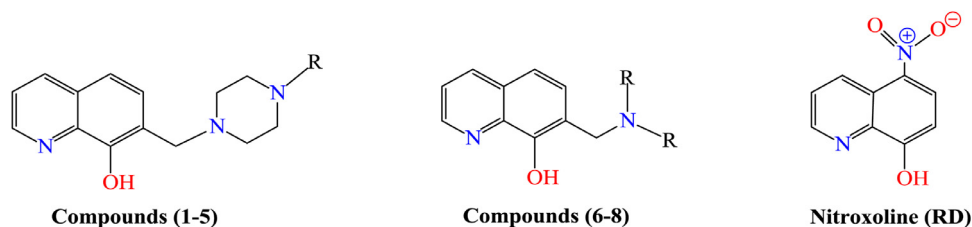


Fig. 1. Molecular structures of antibacterial candidates (1-8) and reference drug (RD).

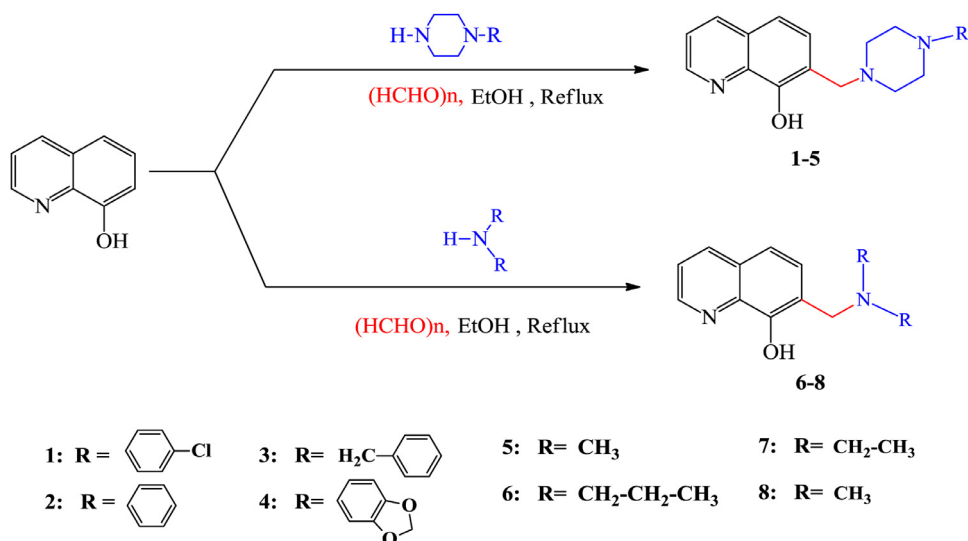


Fig. 2. Scheme of the synthesis route of 7-substituted quinolin-8-ol derivatives 1-8.

## 2. Experimental

### 2.1. General information

Melting points were determined on a Wagner Munz<sup>TM</sup> Kofler Hot Bench. NMR spectra were registered by Bruker Avance (300 MHz) in solutions in (CD<sub>3</sub>)<sub>2</sub>S=O. Elemental C H N Vario Micro Cube analyzer was used in microanalysis. All reagents were analytical quality (Aldrich, Germany). TLC pursued the advancement of the reaction. Column chromatography was done by silica gel (0.040–0.063 mm) by elution with the acetone-hexane mixture.

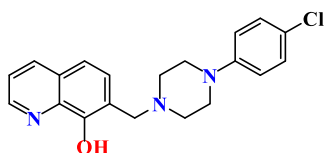
### 2.2. Chemical study

2.2.1. *Synthesis of 7-substituted quinolin-8-ol derivatives.* 7-substituted quinolin-8-ol derivatives were prepared according to the Mannich reaction as mentioned in the literature [23]. The synthesis was performed by the condensation of 8-hydroxyquinoline with secondary amines in refluxed ethanol. The reaction is presented in the following (Fig. 2).

#### 2.2.2. The overall way for the preparation of 7-substituted quinolin-8-ol derivatives

The preparation of 7-substituted quinolin-8-ol derivatives was carried out in two stages. The first one corresponds to the preparation of the Mannich reagent which consists in heating a mixture of secondary amines (0.015 mole), paraformaldehyde (0.66 g, 0.02 mole), and 50 ml of absolute ethanol, until obtaining a clear solution. In a second step, after cooling the reaction mixture previously prepared, (0.015 mole) of quinolin-8-ol suspended in 50 ml of ethanol were added. The reaction mixture is left to stand for 1 hour at room temperature and then heated under reflux of absolute ethanol for an additional 3 h. After evaporation of the ethanol, the residue thus obtained was dissolved in a saturated solution of NaCl, and then made neutral (pH 6 to 7) by the addition of a 2 M aqueous hydrochloric acid solution and extracted with ether (3 × 20 ml). The ethereal phases are combined, dried over anhydrous MgSO<sub>4</sub>, filtered on sintered glass, and evaporated. The resulting residue was purified by column chromatography on silica gel using a mixture of hexane/acetone (9:1 to 3:7, v/v) to get solid with a good to moderate yield for all the synthesized compounds.

#### 2.2.3. Data value, and validation

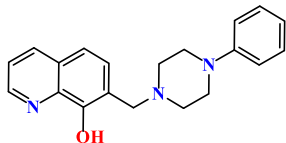


The obtained product (1) is in the form of a brown powder with a yield of 89%, and a melting point between 180 and 182 °C.

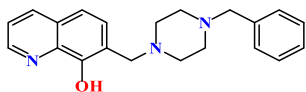
<sup>1</sup>H NMR (300 MHz, (CD<sub>3</sub>)<sub>2</sub>S=O), δ<sub>ppm</sub>: 6.91–8.76 (m, 10H, quinoline et phenyl); 3.62 (s, 2H, quinoline -CH<sub>2</sub>-piperazine); 2.87 (t, 8H, -CH<sub>2</sub>-N of piperazine); 3.12 (t, 4H, -CH<sub>2</sub>-N of piperazine). <sup>13</sup>C NMR (300 MHz, (CD<sub>3</sub>)<sub>2</sub>S=O), δ<sub>ppm</sub>: 53.71, 56.47

(N-CH<sub>2</sub>-C), 60.78 (quinoline-CH<sub>2</sub>-piperazine) ; 111.32, 119.95, 122.29, 127.91, 127.91, 128.95, 129.30, 133.77, 136.37, 138.04, 139.67, 148.37, 152.74 (CH and C of quinoline, and 4-chlorophenyle rings).

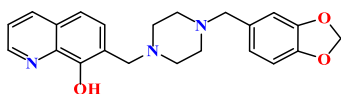
Elemental analysis for C<sub>20</sub>H<sub>20</sub>ClN<sub>3</sub>O, Calcd: C, 67.89; H, 5.70; N, 11.88%. Found: C, 67.88; H, 5.69; N, 11.90%.



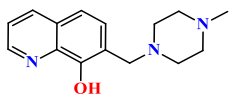
The obtained product (**2**) is in the form of a brown powder with a yield of 85%, and a melting point between 160 and 162 °C. <sup>1</sup>H NMR (300 MHz, (CD<sub>3</sub>)<sub>2</sub>S=O), δ<sub>ppm</sub>: 6.71–8.76 (m, 10 H, quinoline et phenyl); 3.83 (s, 2H, quinoline -CH<sub>2</sub>-piperazine); 2.70 (t, 4H, -CH<sub>2</sub>-N of piperazine); 3.66 (t, 4H, -CH<sub>2</sub>-N of piperazine). <sup>13</sup>C NMR (300 MHz, (CD<sub>3</sub>)<sub>2</sub>S=O), δ<sub>ppm</sub>: 51.37– 55.35 (N-CH<sub>2</sub>-C of piperazine), 59.84 (quinoline-CH<sub>2</sub>-piperazine), 114.59, 123.66, 125.92, 127.84, 128.54, 128.60, 132.77, 134.07, 139.98, 145.07, 146.04, 152.26 (CH and C of quinoline and phenyl rings). Elemental analysis for C<sub>20</sub>H<sub>21</sub>N<sub>3</sub>O, Calcd: C, 75.21; H, 6.63; N, 13.16%. Found: C, 75.22; H, 6.59; N, 13.19%.



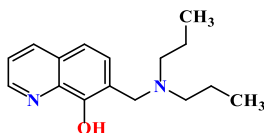
The product obtained (**3**) is in the form of a brown powder with a yield of 83%, and a melting point between 167 and 169 °C. <sup>1</sup>H NMR (300 MHz, (CD<sub>3</sub>)<sub>2</sub>S=O), δ<sub>ppm</sub>: 7.05–8.83 (m, 9H, quinoline and benzyl), 2.28 (s, 4H, quinoline-CH<sub>2</sub>-N and piperazine-CH<sub>2</sub>-benzyl), 3.77 (s, 8H, CH<sub>2</sub> of piperazine). <sup>13</sup>C NMR (300 MHz, (CD<sub>3</sub>)<sub>2</sub>S=O), δ<sub>ppm</sub>: 52.39 (N-CH<sub>2</sub>-C of piperazine), 57.49 (quinoline-CH<sub>2</sub>-piperazine), 62.83 (piperazine -CH<sub>2</sub>-phenyl), 119.95, 122.29, 127.83, 127.91, 128.95, 129.30, 133.77, 136.37, 138.04, 139.67, 148.37, 152.74 (CH and C of quinoline and phenyl rings). Elemental analysis for C<sub>15</sub>H<sub>19</sub>N<sub>3</sub>O, Calcd: C, 70.01; H, 7.44; N, 16.33%. Found: C, 70.04; H, 7.46; N, 16.31%.



The product obtained (**4**) is in the form of a brown powder with a yield of 50%, and a melting point between 210 and 212 °C. <sup>1</sup>H NMR (300 MHz, (CD<sub>3</sub>)<sub>2</sub>S=O), δ<sub>ppm</sub>: 6.82–8.76 (m, 8H, aromatique and benzo [1.3] dioxole), 3.05 (s, 2H, aromatique-CH<sub>2</sub>-N and piperazine-CH<sub>2</sub>-benzo [1.3] dioxole), 2.28 (s, 8H, -CH<sub>2</sub>-piperazine), 3.76 (s, 2H, piperazine -CH<sub>2</sub>-phényle), 6.97–7.11 (m, 3H, -CH-), 5.91 (s, 2H, CH<sub>2</sub> of dioxole). <sup>13</sup>C NMR (300 MHz, (CD<sub>3</sub>)<sub>2</sub>S=O), δ<sub>ppm</sub>: 64.12 (piperazine-CH<sub>2</sub>-benzo [1.3] dioxole), 58.02 (CH<sub>2</sub> of piperazine), 53.49 (quinoléine-CH<sub>2</sub>-piperazine), 64.27 (N-CH<sub>2</sub>-1-(benzo [1.3] dioxole), 101.18, 108.23, 109.46, 120.83, 121.81, 122.33, 124.60, 128.28, 129.19, 132.46, 134.17, 139.27, 146.53, 147.616, 148.18, 153.21 (CH and C of quinoline and benzo [1.3] dioxole rings). Elemental analysis for C<sub>22</sub>H<sub>23</sub>N<sub>3</sub>O<sub>3</sub>, Calcd: C, 70.01; H, 6.14; N, 11.13%. Found: C, 70.07; H, 6.10; N, 11.12%.

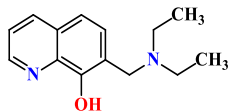


The product obtained (**5**) is in the form of a brown powder with a yield of 90%, and a melting point between 140 and 142 °C. <sup>1</sup>H NMR (300 MHz, (CD<sub>3</sub>)<sub>2</sub>S=O), δ<sub>ppm</sub>: 7.01–8.85 (m, 5H, quinoline), 3.65 (s, 2H, quinoléine -CH<sub>2</sub>-N), 1.70 (s, 3H, -CH<sub>3</sub>), 2.08 (t, 4H, CH<sub>2</sub> of piperazine), 2.89 (t, 4H, CH<sub>2</sub> of piperazine). <sup>13</sup>C NMR (300 MHz, (CD<sub>3</sub>)<sub>2</sub>S=O), δ<sub>ppm</sub>: 45.08 (CH<sub>3</sub>); 55.17, 60.14 (N-CH<sub>2</sub>-C of piperazine), 61.35 (quinoline-CH<sub>2</sub>-piperazine), 121.70, 122.20, 127.85, 129.08, 134.21, 136.41, 148.17, 148.54, 153.71 (CH and C of quinoline ring). Elemental analysis for C<sub>15</sub>H<sub>19</sub>N<sub>3</sub>O, Calcd: C, 70.01; H, 7.44; N, 16.33%. Found: C, 70.03; H, 7.41; N, 16.34%.

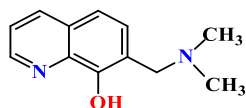


The product obtained (**6**) is in the form of a green powder with a yield of 70%, and a melting point between 162 and 164 °C. <sup>1</sup>H NMR (300 MHz, (CD<sub>3</sub>)<sub>2</sub>S=O), δ<sub>ppm</sub>: 7.03–8.86 (m, 5H, quinoline), 2.38 (t, 2H, N-CH<sub>2</sub>), 1.14 (s, 2H, -CH<sub>2</sub>-), 3.69 (s,

2H, quinoline-CH<sub>2</sub>-N), 0.77 (t, 3H, CH<sub>3</sub>), <sup>13</sup>C NMR (300 MHz, (CD<sub>3</sub>)<sub>2</sub>S=O), δ<sub>ppm</sub>: 13.228 (CH<sub>3</sub>), 27.840 (CH<sub>2</sub>), 46.47 (CH<sub>2</sub>-N), 55.59 (quinoline-CH<sub>2</sub>-N), 110.22, 121.54, 128.75, 133.99, 147.99, 125.91, 128.75, 139.40, 153.03 (CH and C of quinoline ring). Elemental analysis for C<sub>16</sub>H<sub>22</sub>N<sub>2</sub>O, Calcd: C, 74.38; H, 8.58; N, 10.84%. Found: C, 74.36; H, 8.61; N, 10.86%.



The product obtained (**7**) is in the form of a green powder with a yield of 82%, and a melting point between 131 and 133 °C. <sup>1</sup>H NMR (300 MHz, (CD<sub>3</sub>)<sub>2</sub>S=O), δ<sub>ppm</sub>: 7.009–8.857 (m, 5H, quinoline ring), 3.655 (s, 2H, quinoline-CH<sub>2</sub>-N), 2.027 (s, 3H, -CH<sub>3</sub>). <sup>13</sup>C NMR (300 MHz, (CD<sub>3</sub>)<sub>2</sub>S=O), δ<sub>ppm</sub>: 14.51(CH<sub>3</sub>), 49.38(-CH<sub>2</sub>-) 62.04 (quinoline ring -CH<sub>2</sub>-N), 121.44, 125.05, 128.20, 129.98, 148.10, 130.13, 134.07, 139.22, 153.28 (CH and C of quinoline ring). Elemental analysis for C<sub>14</sub>H<sub>18</sub>N<sub>2</sub>O, Calcd: C, 73.01; H, 7.88; N, 12.16%. Found: C, 73.02; H, 7.85; N, 12.19%.



The product obtained (**8**) is in the form of a green powder with a yield of 90%, and a melting point between 112 and 114 °C. <sup>1</sup>H NMR (300 MHz, (CD<sub>3</sub>)<sub>2</sub>S=O), δ<sub>ppm</sub>: 4.64 (s, 2H, quinoline ring-CH<sub>2</sub>-N), 1.95(s, 3H, CH<sub>3</sub>), 7.03–8.86 (m, 5 H, quinoline ring). <sup>13</sup>C NMR (300 MHz, (CD<sub>3</sub>)<sub>2</sub>S=O), δ<sub>ppm</sub>: 62.83 (quinoline ring -CH<sub>2</sub>-N), 111.12, 120.37, 122.04, 128.48, 148.59, 131.20, 134.01, 138.98, 154.15 (C and CH of quinoline ring), 42.75 (CH<sub>3</sub>). Elemental analysis for C<sub>12</sub>H<sub>14</sub>N<sub>2</sub>O, Calcd: C, 71.26; H, 6.98; N, 13.85%. Found: C, 71.22; H, 7.00; N, 13.88%.

All the spectral characterization data of 7-substituted quinolin-8-ol derivatives are gathered in the Supplementary file.

## 2.3. Pharmacological screening

### 2.3.1. Microorganisms

The bacterial strains used in this study are frequent in human pathology, they are two Gram-positive bacteria (*Staphylococcus aureus*, *Bacillus subtilis*), and two to Gram-negative (*Escherichia coli*, *Enterobacter ludwigii*). The used microorganisms were supplied through the Laboratory of Nutrition, Health, and Environment, Faculty of Sciences, Ibn Tofail University, Kenitra, Morocco.

### 2.3.2. Antibacterial assay

Antibacterial evaluation of the synthesized 7-substituted quinolin-8-ol derivatives has been performed by the disc method. In this technique, bacteria were streaked onto Petri dishes including Muller Hinton agar. Sterile blank disks (6 mm in diameter) were saturated with a solution of 100 μg/mL of synthesized compounds solubilized in 1% of dimethyl sulfoxide (DMSO) and following; all discs were incubated at 37 °C for 24 h. The development obtained of inhibition zones were compared with those of reference disks. Nitroxoline was used as a standard reference drug and DMSO as a control.

### 2.3.3. Minimum inhibitory concentration (MIC)

The MICs were decided through the serial dilution method according to the standard procedure [24]; it consists of bringing a standardized bacterial inoculum into contact with increasing concentrations of the synthesized 7-substituted quinolin-8-ol derivatives. After 24 h of incubation at 37 °C, the MIC obtained corresponds to the concentration at which the inhibition of bacterial growth is visible to the naked eye (absence of turbidity in the tube).

### 2.3.4. Molecular docking

The molecular docking of the compounds (**1–8** and standard drug Nitroxoline) was achieved through iGEMDOCK (BioXGEM, Taiwan). Crystal coordinates of the FtsZ from *Staphylococcus aureus* (SaFtsZ) in complex with PC190723 inhibitor (PDB ID: 9 PC) were acquired from the Protein Data Bank (PDB, <https://www.rcsb.org/>, PDB: 3VOB). In the first step, the structure of SaFtsZ was developed, comprising the removal of H<sub>2</sub>O molecules and optimized protein structure using BIOVIA Discovery Studio 4.5 (Dassault Systèmes, France). The 3D structures of eight 7-substituted quinolin-8-ol derivatives were optimized using the molecular mechanics force field (MM+) [25], and subsequently by the semiempirical PM3 method [26] using the Avogadro 1.2.0. (University of Pittsburgh, Pittsburgh, PA, USA). Once having prepared the target protein, and global of optimized structures of 4 compounds as ligands, genetic parameters were set (population size: 300; generations: 70; number of poses: 5). Binding site (radius 8 Å) was chosen by the PC190723 ligand (3-[(6-chloro[1,3]thiazolo[5,4-b]pyridin-2-yl)methoxy]-2,6-difluorobenzamide) [19].

**Table 1**

Zone of growth inhibition of 7-substituted quinolin-8-ol derivatives, and Nitroxoline against various studied bacteria.

Compound	Inhibition zone diameter (mm)			
	Gram-positive bacteria		Gram-negative bacteria	
	<i>B. subtilis</i>	<i>S. aureus</i>	<i>E. coli</i>	<i>E. ludwigii</i>
<b>1</b>	<b>42</b>	<b>30</b>	<b>52</b>	<b>48</b>
<b>2</b>	28	26	28	<b>30</b>
<b>3</b>	22	23	25	25
<b>4</b>	No zone	8	12	No zone
<b>5</b>	16	14	24	<b>30</b>
<b>6</b>	12	12	12	12
<b>7</b>	9	9	No zone	No zone
<b>8</b>	No zone	No zone	No zone	No zone
<b>Nitroxoline</b>	<b>30</b>	20	32	17
<b>DMSO</b>	No zone	No zone	No zone	No zone

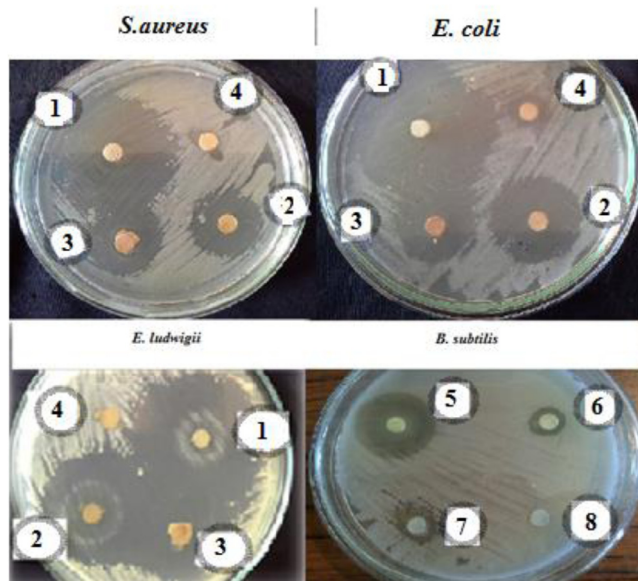


Fig. 3. Some antibiograms obtained for 7-substituted quinolin-8-ol derivatives.

Each compound in the library was docked into the binding site, and protein–compound interaction profiles of electrostatic (Elec), hydrogen-bonding (H-bond), and vdW interactions were established. Finally, the organic molecules were classified through a combination of the pharmacological interactions, and energy-based scoring function. Energy-based scoring function or total energy ( $E$ ) is:  $E = \text{vdW} + \text{Hbond} + \text{Elec}$  [27].

### 3. Results and discussion

#### 3.1. Synthesis and bioactivity

The compounds synthesized were obtained with very good yields, except compound 7-((4-(benzo [1,3] dioxol –5-ylmethyl) piperazin-1-yl) methyl) quinolin-8-ol (**4**), which is obtained with a yield of 50%. This low yield can be explained by a steric gene due to the large size of the C-7 substituent of quinolin-8-ol.

However, the diameters of the inhibition zone (in millimeters) for the 7-substituted quinolin-8-ol derivatives against four bacterial strains used are indicated in Table 1, and Fig. 3. Nonetheless, selecting Nitroxoline as a reference drug relies on the fact that its structure extremely near that of the evaluated compounds. However, it is well known that the molecule is considered to be inactive if it produces diameters of inhibition less than or equal to 8 mm, intermediate for diameters between 8 and 14 mm. It is moderately effective for a diameter between 14 and 20 mm and for a diameter greater than or equal to 20 mm the molecule is very effective. The obtained data reveal that products **1**, **2**, **3**, and **5** were the more active of all synthesized molecules with growth inhibition zones 52, 28, 25, and 24 mm, respectively, at 100  $\mu\text{g}/\text{mL}$  against *E. coli*, compared to the standard drug Nitroxoline (32 mm) at 100  $\mu\text{g}/\text{mL}$ . Compounds **1**, **2**, **3**, and **5** exhibited significantly

**Table 2**  
The MICs in  $\mu\text{g/ml}$  of 7-substituted quinolin-8-ol derivatives **1–8**.

Compound	Antibacterial activity (MIC in $\mu\text{g/ml}$ )			
	<i>B. subtilis</i>	<i>S. aureus</i>	<i>E. coli</i>	<i>E. ludwigii</i>
<b>1</b>	20	<b>10</b>	<b>10</b>	<b>10</b>
<b>2</b>	40	20	20	<b>10</b>
<b>3</b>	50	40	<b>10</b>	<b>10</b>
<b>4</b>	—	100	70	—
<b>5</b>	<b>10</b>	60	40	20
<b>6</b>	60	90	90	80
<b>7</b>	60	100	80	80
<b>8</b>	—	—	—	—
<b>Nitroxoline</b>	20	<b>10</b>	<b>10</b>	<b>10</b>

**Table 3**  
Docking score energy of interactions of the best-docked poses of 7-substituted quinolin-8-ol derivatives in complex with FtsZ.

Compound (pose)	Total energy/Kcal mol <sup>-1</sup>	Van der Waals interaction/kcal mol <sup>-1</sup>	H Bond/Kcal mol <sup>-1</sup>
<b>3 (1)</b>	-131.31	-125.38	-5.93
<b>PC190723 (3)</b>	-121.89	-103.41	-18.48
<b>4 (1)</b>	-118.41	-110.88	-7.53
<b>2 (3)</b>	-114.82	-111.44	-3.38
<b>1 (3)</b>	-114.73	-111.98	-2.75
<b>5 (2)</b>	-105.45	-94.95	-10.50
<b>6 (3)</b>	-105.36	-97.02	-8.34
<b>7 (3)</b>	-98.09	-89.37	-8.72
<b>Nitroxoline (3)</b>	-94.44	-69.66	-24.78
<b>8 (0)</b>	-90.40	-83.50	-6.90

stronger antibacterial activity than the standard Nitroxoline drug for all the microorganisms tested, while **4** and **6** compounds showed moderate activity against all microorganisms tested. The increase in antibacterial activity can be attributed to the presence of aromatic substitutions at the piperazine cycle in position 7. Thus, the compounds with the piperazine cycle in position 7 have a higher antibacterial activity than the compounds carrying amines secondary. However, Compound 5 with the methylpiperazine substituent showed moderate activity against Gram-positive and Gram-negative bacteria. On the other hand, compound **6** is more active than compounds **7** and **8**, which shows that the alkyl chain length on the nitrogen atom has an important role in the antibacterial activity.

Thereafter, the results of the MIC evaluation for all synthesized compounds and the Nitroxoline are summarized in Table 2.

The MIC values of compounds **1**, **2**, **3**, **4**, and **5** having piperazine substituted in C-7, against *S. aureus* bacterial strain are respectively 10, 20, 40, 100 and 60  $\mu\text{g/ml}$ , while against the *B. subtilis*, compounds **1**, **2**, **3** and **5** inhibited bacterial growth with MIC values of 20, 40, 50 and 10  $\mu\text{g/ml}$  respectively. On the other hand, compound **4** exhibited no antibacterial activity. The compounds **1**, **2**, **3**, **4**, and **5** exhibited 10, 20, 10, 70, 40  $\mu\text{g/ml}$  MIC values against *E. coli*, respectively. Further, the tested compounds (**1**, **2**, **3**, and **5**) against *E. ludwigii* exhibited MIC ranging between 10  $\mu\text{g/ml}$  and 20  $\mu\text{g/ml}$ . However, among the derivatives carrying the secondary amines with saturated chain (**6**, **7**, and **8**), only compound **6** showed MIC values of 60, 90, 90, and 80  $\mu\text{g/ml}$  against *B. subtilis*, *S. aureus*, *E. coli*, and *E. ludwigii*, respectively. Consequently, it can be noted that the grafting of long saturated secondary chain amines makes it possible to modify the antibacterial potential; as well as a piperazine cycle carrying electron donor substituents can also increase biological activity.

### 3.2. Docking study

Table 3 presents the best nine docking scores ranked by the energy-based scoring function and their energy interactions. The results are in agreement with the antibacterial activity assays. The highest-ranked is compound **3**, in docking pose **1** has the lowest total energy ( $-131.31 \text{ kcal mol}^{-1}$ ), which also demonstrated good antibacterial activity against *S. aureus*, same as compound **2** ( $-114.82 \text{ kcal mol}^{-1}$ ) and compound **1** ( $-114.73 \text{ kcal mol}^{-1}$ ) (Tables 2 and 3). Inhibitor PC190723, which has potent and selective antistaphylococcal activity, was secondranked, immediately after compound **3** ( $-121.89 \text{ kcal mol}^{-1}$ ). Nitroxoline, an antibacterial drug, exhibited low binding affinities to the FtsZ protein (total energy:  $-100.82$  and  $-94.44 \text{ kcal mol}^{-1}$ , respectively), which confirms the results of the antibacterial assay. Compound **8** exhibited the lowest binding potential ( $-90.40 \text{ kcal mol}^{-1}$ ) and also, did not show a zone of growth inhibition against *S. aureus*.

Energies of the main interactions between SaFtsZ residues, and ligand **3** are listed in Table 4. Interactions of other compounds were joined in Supplementary file 1 (SF 1).

**Table 4**

Energies of the main interactions SaFtsZ residues, and ligand **3** (*M* = main chain; *S* = side chain, *H* = Hydrogen bond; *V* = van der Waals interaction).

Residual	Energy of interaction
H-M-GLN-192	-3.62
H-S-THR-309	-2.31
V-M-GLN-192	-5.43
V-S-GLN-192	-2.40
V-M-GLY-193	-7.10
V-M-GLY-196	-7.38
V-M-ASP-199	-4.17
V-M-LEU-200	-9.96
V-S-LEU-200	-5.01
V-M-VAL-203	-3.77
V-M-GLY-227	-6.20
V-S-ASN-263	-9.83
V-S-VAL-297	-4.99
V-M-THR-309	-3.49
V-M-VAL-310	-4.18

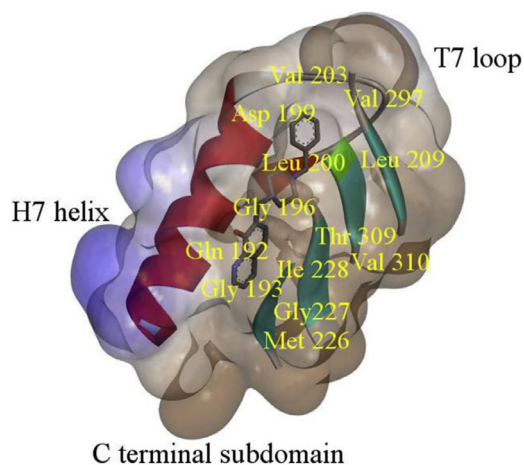


**Fig. 4.** The hydrophobic surface of binding site SaFtsZ in complex with compound **3**. (Hydrophobicity is ranged from  $-3.0$  (blue) to  $0.0$  (white) and to the  $3.0$  (brown).

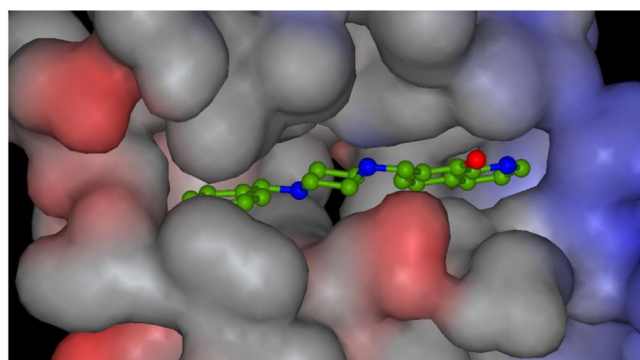


**Fig. 5.** Electrostatic potential surface representation of SaFtsZ binding site with docked compound **3**. (Range of potential: from min.  $1.77$  mV (blue) to the max.  $0.541$  mV (red)).

Similar to ligand PC19072, compound **3** binds to the hydrophobic cleft located between the H7 helix, and the C-terminal subdomain of SaFtsZ (Fig. 3) [19]. Fig. 4 shows the docking interactions of ligand **3** at the PC190723-binding site of SaFtsZ. Electrostatic potential surface representation of SaFtsZ binding site with docked compound **4a** is presented in Figs. 5 and 6.

The benzyl group is located in the hydrophobic core generating the interactions with residues: Leu200 ( $3.98$  Å), Val297 ( $3.42$  Å), and Val203 ( $5.15$  Å), while the piperazin-1-yl group forms alkyl interaction with Leu200 ( $4.48$  Å). The two fluoro groups of PC190723 were located in the internal space surrounded by the same residues [19]. These structural features,



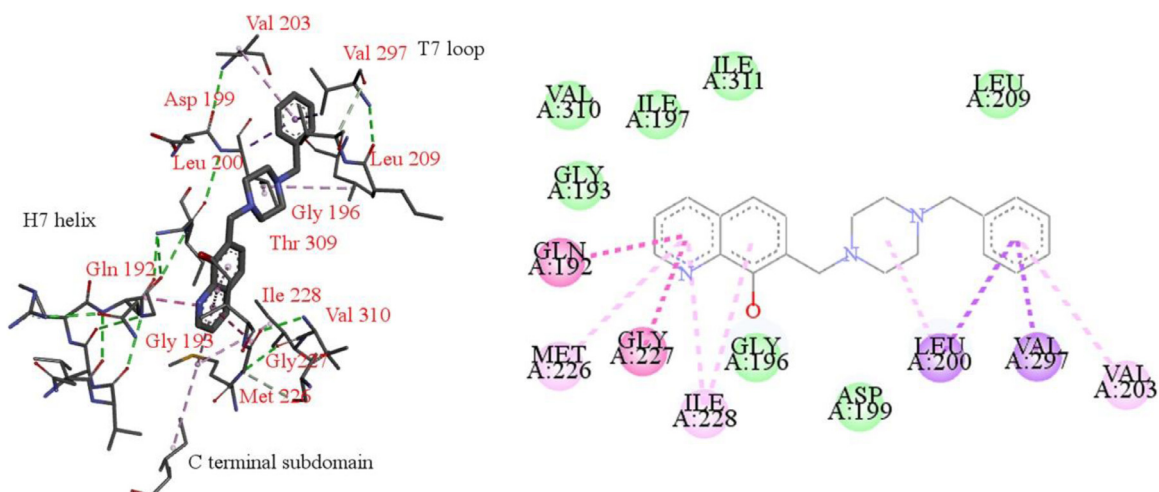


**Fig. 6.** a) Docking of compound **3** in the best pose at the PC190723-binding site of FtsZ from *Staphylococcus aureus* (PDB:3VOB); b) 2D representation of interactions. (light green: van der Waals, green: hydrogen bond; dark purple:  $\pi$ - $\sigma$  interactions; purple:amide- $\pi$  interactions, light purple: alkyl, and  $\pi$ -alkyl interactions).

which possess compounds **1–5**, could be key for the enhanced binding affinity toward FtsZ, and also for the inhibition of bacterial growth. Compounds **6–8** are lacked by these substituents and they do not have the possibility for strong interactions with residues of T7 loop (Fig. 6a and b). Therefore, these compounds showed lower binding affinity and weak inhibition against *S. aureus*.

The quinolin-8-ol moiety of compound **3** is located, as the thiazolopyridine moiety of PC190723, in a hydrophobic cleft between the H7 helix, and the C-terminal subdomain formed by amino-acid residues Gly193, Gly196, Ile197, Thr309, and Ile331. The pyridine ring of quinoline interacts through the amide- $\pi$  interactions with Gln192 (3.79 Å), and Gly227 (4.21 Å), as well as with Met226 (4.66 Å), and Ile228 (5.34 Å) by the  $\pi$ -alkyl interactions. It has been shown that binding of PC190723 to the cleft located fixes the movement and may prevent the active residues in the T7 loop from being located at the appropriate site for the GTPase activity [19]. Since molecule **3** has a similar binding mode at the FtsZ binding site as the PC190723 inhibitor, which has expressed antistaphylococcal activity, it is a promising candidate for medicine against *Staphylococcus aureus*.

### 3.3. POM theory application for identification of pharmacophore sites

A potential drug, should not have only good bioactivity, it must have acceptable pharmacokinetic properties. To reach the pharmacokinetic activity of molecules, we utilized Osiris, Petra, and Molinspiration (POM) as a good virtual screening with about 7000 drugs available on the market. It is of great importance to be able to identify the type of pharmacophore site each clinical drug contains. To reply to this query, we developed POM Theory in the goal to elucidate between antibacterial [28–36], antifungal [37–52], antiviral [53–55], antitumoral [56–68], antiparasitic [69], drugs, and various enzymes inhibitors [70–72]. The POM Theory was invented by Prof T. Ben Hadda based on the most important descriptors:

- 1- The geometry of pharmacophore sites.
- 2- Type of 3D interaction of drugs with specific biotargets.
- 3- The electrostatic drug/biotarget interaction.

So, we will analyze a series of compounds by using Petra/Osiris/Molinspiration (POM) bioinformatic platform-2019 [28–72].

#### 3.3.1. Atomic charge, and Osiris calculations

The atomic charge, and Osiris calculations (Fig. 7, Table 5), indicate the presence of the antibacterial ( $N^{\delta-}$  – – –  $OH^{\delta+}$ ) pharmacophore site, as it was postulated based on fundamental concepts of POM theory which were invented by Taïbi Ben Hadda group's [27–72].

#### 3.3.2. Osiris calculations

Osiris analysis of the reference drug (RD = Nitroxoline), and the tested molecules **1–8** revealed that derivatives of quinolin-8-ol, contrary to the reference drug, represent a good and high drug-likeness (DL = 1.97–8.04), and (DL = –6.95) respectively for series **1–8** and Reference drug, as given in Fig. 8, and Table 6.

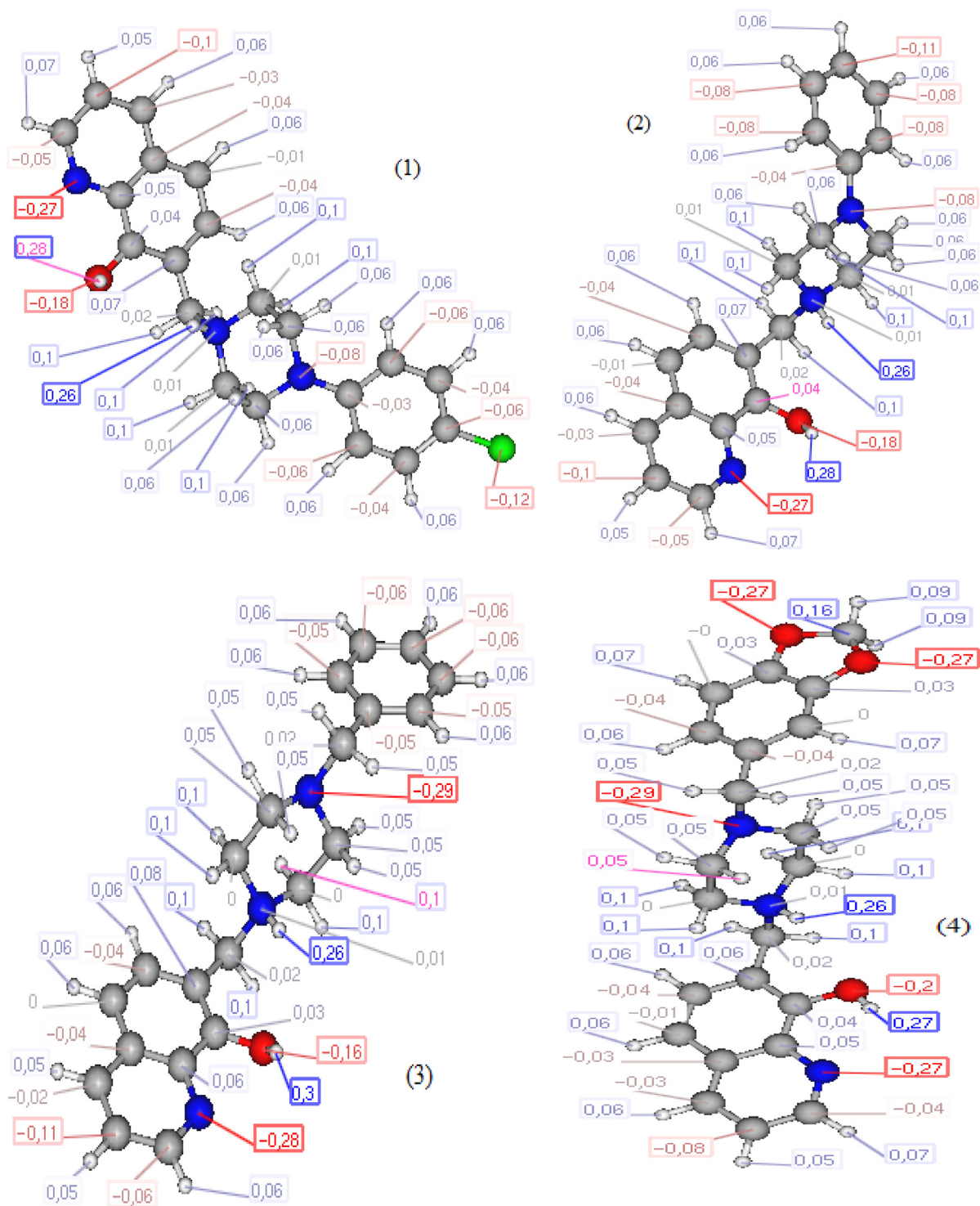
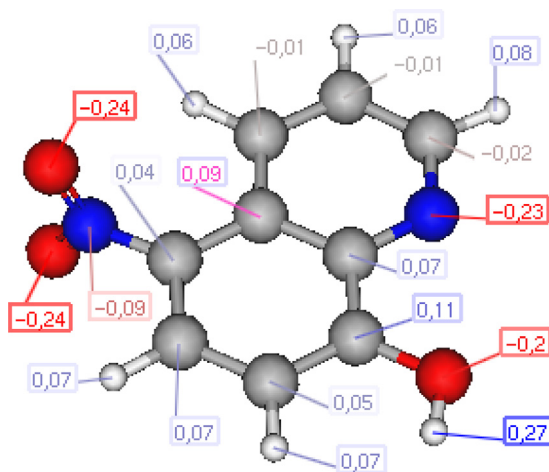


Fig. 7. Atomic Charges of compounds (1–8) and reference drug (RD).





Nitroxoline (RD)

Fig. 7. Continued

**Table 5**  
Atomic charge calculations of compounds 1–8.

Compound	Atomic charge				Antibacterial pharmacophore site
	R	N(1)	N(1)H(1)	O(1)	
1		-0.27	0.28	-0.18	N(1)...HO(1)
2		-0.27	0.28	-0.18	N(1)...HO(1)
3		-0.28	0.30	-0.18	N(1)...HO(1)
4		-0.27	0.27	-0.20	N(1)...HO(1)
5	---CH <sub>3</sub>	-0.28	0.30	-0.18	N(1)...HO(1)
6	---C <sub>3</sub> H <sub>7</sub>	-0.28	0.30	-0.16	N(1)...HO(1)
7	---C <sub>2</sub> H <sub>5</sub>	-0.28	0.30	-0.16	N(1)...HO(1)
8	---CH <sub>3</sub>	-0.28	0.30	-0.16	N(1)...HO(1)
RD	-----	-0.23	0.27	-0.20	N(1)...HO(1)

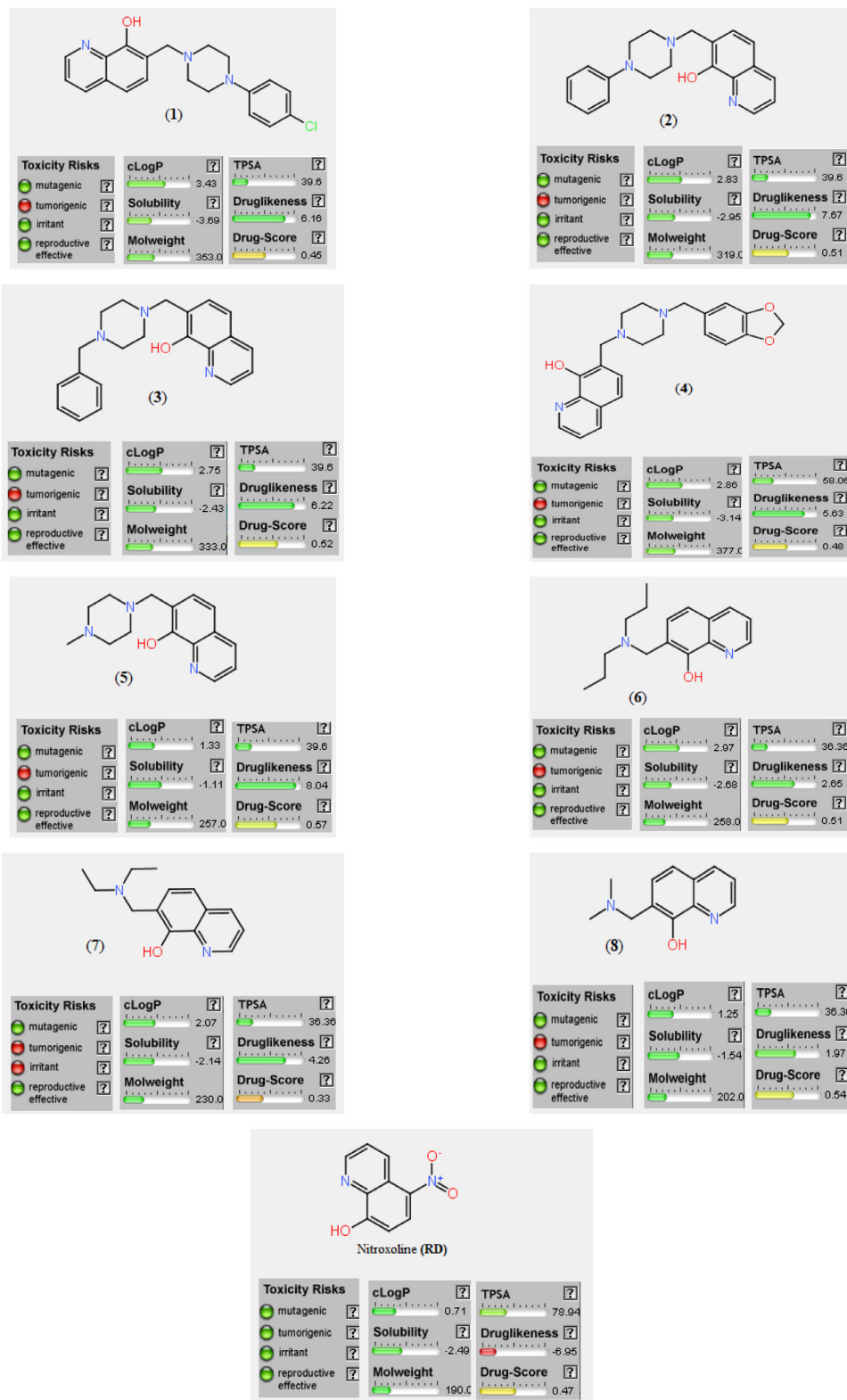


Fig. 8. Osiris calculations of compounds (1–8), and reference drug (RD).

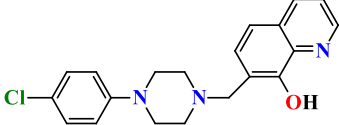
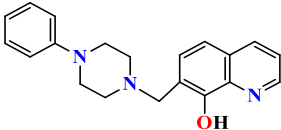
**Table 6**  
Osiris calculations of toxicity risks, and drug score of 7-substituted quinolin-8-ol (**1–8**).

Compound	MW	Toxicity Risks <sup>[a]</sup>				Drug Score Calculations <sup>[b]</sup>			
		MUT	TUM	IRRI	REP	cLogP	cLogS	DL	DS
<b>1</b>	353	+++	–	+++	+++	3.43	–3.69	6.16	0.45
<b>2</b>	319	+++	–	+++	+++	2.83	–2.95	7.67	0.51
<b>3</b>	333	+++	–	+++	+++	2.75	–2.43	6.22	0.52
<b>4</b>	377	+++	–	+++	+++	2.86	–3.14	5.63	0.48
<b>5</b>	257	+++	–	+++	+++	1.33	–1.11	8.04	0.57
<b>6</b>	258	+++	–	+++	+++	2.97	–2.68	2.65	0.51
<b>7</b>	230	+++	–	–	+++	2.07	–2.14	4.26	0.33
<b>8</b>	202	+++	–	+++	+++	1.25	–1.54	1.97	0.54
<b>RD</b>	190	+++	+++	+++	+++	0.71	–2.49	–6.95	0.47

Not toxic (+++), highly toxic: (–), slightly toxic: (+). <sup>[a]</sup> RE: Reproductive effective, IRRIT: Irritant, TUM: Tumorigenic, MUT: Mutagenic. <sup>[b]</sup> DS: Drug-Score, DL: Drug Likeness, Sol: Solubility.

They showed better drug scores and can be utilized as therapeutic agents. Structures of the investigated antibacterial drugs are supposed to present some risks when running through the mutagenicity, but these compounds were at low risk compared with compound **7** as irritation, and tumorigenic effects are concerned.

**Table 7**  
Molinspiration calculations of 7-substituted quinolin-8-ol derivatives (**1–8**).

Compound	Molecular Properties	Bioactivity Scores	
 <p style="text-align: center;"><b>(1)</b></p>	miLogP	3.70	
	TPSA	40	
	natoms	25	
	MW	354	
	nON	4	
	nOHNH	1	
	nviolations	0	
	nrotb	3	
	volume	316	
		GPCR ligand	0.13
	Ion channel modulator	0.06	
	Kinase inhibitor	0.24	
	Nuclear receptor ligand	–0.17	
	Protease inhibitor	–0.06	
	Enzyme inhibitor	0.07	
 <p style="text-align: center;"><b>(2)</b></p>	miLogP	3.02	
	TPSA	40	
	natoms	24	
	MW	319	
	nON	4	
	nOHNH	1	
	nviolations	0	
	nrotb	3	
		GPCR ligand	0.14
		Ion channel modulator	0.07
	Kinase inhibitor	0.27	
	Nuclear receptor ligand	–0.16	
	Protease inhibitor	–0.02	

(continued on next page)

Table 7 (continued)

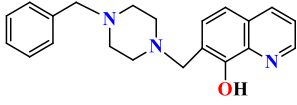
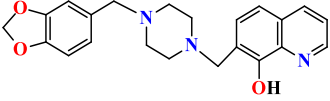
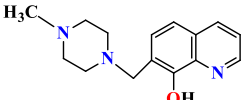
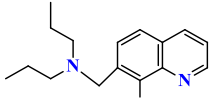
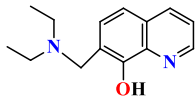
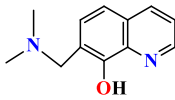
	<u>volume</u>	302	Enzyme inhibitor	0.11
 <p>(3)</p>	<u>miLogP</u>	2.72		
	<u>TPSA</u>	40		
	natoms	25		
	MW	333	GPCR ligand	0.12
	nON	4	Ion channel modulator	0.08
	nOHNH	1	Kinase inhibitor	0.24
	nviolations	0	Nuclear receptor ligand	-0.12
	nrotb	4	Protease inhibitor	0.05
	<u>volume</u>	319	Enzyme inhibitor	0.17
	 <p>(4)</p>	<u>miLogP</u>	2.61	
<u>TPSA</u>		58		
natoms		28	GPCR ligand	0.09
MW		377	Ion channel modulator	-0.02
nON		6	Kinase inhibitor	0.15
nOHNH		1	Nuclear receptor ligand	-0.18
nviolations		0	Protease inhibitor	-0.01
nrotb		4	Enzyme inhibitor	0.12
<u>volume</u>		343		
 <p>(5)</p>		<u>miLogP</u>	1.32	
	<u>TPSA</u>	40		
	natoms	19	GPCR ligand	0.07
	MW	257	Ion channel modulator	0.16
	nON	4	Kinase inhibitor	0.26
	nOHNH	1	Nuclear receptor ligand	-0.33
	nviolations	0	Protease inhibitor	-0.15
	nrotb	2	Enzyme inhibitor	0.22
	<u>volume</u>	247		
	 <p>(6)</p>	<u>miLogP</u>	3.19	
<u>TPSA</u>		36		
natoms		19	GPCR ligand	0.06
MW		258	Ion channel modulator	0.11

Table 7 (continued)

	nON 3 nOHNH 1 nviolations 0 nrotb 6 <u>volume</u> 262	Kinase inhibitor 0.13 Nuclear receptor ligand -0.25 Protease inhibitor -0.13 Enzyme inhibitor 0.20
 <b>(7)</b>	<u>miLogP</u> 2.18 <u>TPSA</u> 36 natoms 17 MW 230 nON 3 nOHNH 1 nviolations 0 nrotb 4 <u>volume</u> 228	GPCR ligand -0.13 Ion channel modulator 0.06 Kinase inhibitor 0.03 Nuclear receptor ligand -0.46 Protease inhibitor -0.35 Enzyme inhibitor 0.14
 <b>(8)</b>	<u>miLogP</u> 1.43 <u>TPSA</u> 36 natoms 15 MW 202 nON 3 nOHNH 1 nviolations 0 nrotb 2 <u>volume</u> 195	GPCR ligand -0.25 Ion channel modulator 0.12 Kinase inhibitor 0.01 Nuclear receptor ligand -0.78 Protease inhibitor -0.43 Enzyme inhibitor 0.14
<b>RD</b>	<u>miLogP</u> 1.89 <u>TPSA</u> 78.94 natoms 14 MW 190.16 nON 5 nOHNH 1 nviolations 0 nrotb 1 <u>volume</u> 155.23	GPCR ligand -0.61 Ion channel modulator -0.04 Kinase inhibitor -0.37 Nuclear receptor ligand -0.66 Protease inhibitor -0.99 Enzyme inhibitor -0.09



**Table 8**  
Molinspiration calculations of Lipinski parameters, and Drug-likeness of **1–8**.

Compound	Lipinski parameters calculations <sup>a</sup>				Drug-likeness <sup>b</sup>					
	TPSA	NONH	NV	VOL	GPCRL	ICM	KI	NRL	PI	EI
<b>1</b>	40	1	0	316	0.13	0.06	0.24	-0.17	-0.06	0.07
<b>2</b>	40	1	0	302	0.14	0.7	0.27	-0.16	-0.02	0.11
<b>3</b>	40	1	0	319	0.12	0.07	0.24	-0.12	0.05	0.17
<b>4</b>	58	1	0	343	0.09	-0.02	0.15	-0.18	-0.01	0.12
<b>5</b>	40	1	0	247	0.07	0.16	0.26	-0.33	-0.15	0.22
<b>6</b>	36	1	0	228	-0.13	0.06	0.03	-0.46	-0.35	0.14
<b>7</b>	36	1	0	228	-0.13	0.06	0.03	-0.46	-0.35	0.14
<b>8</b>	36	1	0	195	-0.25	0.12	0.01	-0.78	-0.43	0.14
<b>RD</b>	79	1	0	155	-0.61	-0.04	-0.37	-0.66	-0.99	-0.09

<sup>a</sup> VOL: volume, NONH: number of OH–N or O–NH interaction, TPSA: Total molecular polar surface area, NV: number of violation of five Lipinsky rules.

<sup>b</sup> EI: Enzyme inhibitor, PI: Protease inhibitor, NRL: Nuclear receptor ligand, GPCRL: GPCR ligand; ICM: Ion channel modulator; KI: Kinase inhibitor.

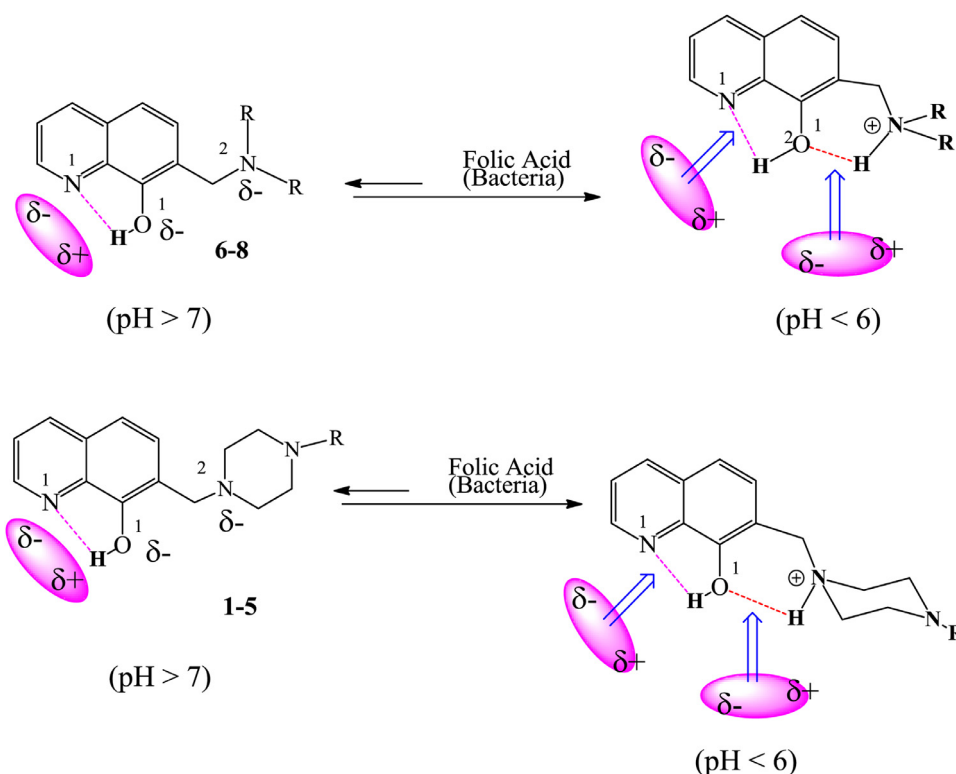


**Fig. 9.** A plausible mechanism of in situ regeneration of two combined synergistic antibacterial ( $N^{\delta-} \text{---}O1H^{\delta+}$ ), and ( $O1^{\delta-} \text{---}N2H^{\delta+}$ )-pharmacophore sites.

### 3.3.3. Moliolinspiration calculations

The Lipinski parameters of each compound (Tables 7 and 8) had been stated in terms of its violation number (n violations) since it had been recognized that the absorption or permeation is importantly affected by this quantity (value of  $cLogP$ ). Therefore, when the value of violations is greater than 4, the bioavailability (absorption or permeation) diminishes. Our results showed that the new compounds (**1–8**) have acceptable  $cLogP$  ( $cLogP < 5$ ). As the molecular weight of all molecules (**1–8** and **RD**) is  $190\text{--}353 > 500$  g/mole, it is necessary to introduce more ramifications chemical (glycosylation) for the purpose of making more potentially active analogs. The actual drug-scores of compounds **1–8** are very encouraging (positive value of DS); most of the compounds **1–8** present good bioactivity scores (Table 8).

#### 4. How do quinolin-8-ol derivatives work?

The pharmacophore sites of the synthesized compounds are shown in Fig. 9, which clearly shows that if the reference drug processes one limited antibacterial pharmacophore site, the series of new compounds process two combined synergistic antiviral pharmacophore sites.

For this reason, this series constitutes an excellent model to use in our next investigation in drug design for more efficient, and selective therapeutic agents.

#### 5. Conclusion

In summary, a series of eight 7-substituted quinolin-8-ol derivatives were successfully prepared in good yields via an easy, handy, and efficient synthetic route. Their structures were identified using  $^1\text{H}/^{13}\text{C}$  NMR spectroscopy, and elemental analysis. These newly synthesized compounds were assessed for antimicrobial activity. Some synthesized compounds exhibited significant antibacterial activities against studied bacterial strains. In particular, compounds 1 and 2 have shown superior antibacterial efficacies compared to that of nitroxoline. In addition, the antibacterial effect of these compounds depends on their chemical structure and on the nature of the substituent carried by the quinolin-8-ol ring. The molecular docking study and the antibacterial test have demonstrated that compound 3 is a promising candidate as an antibacterial against *Staphylococcus aureus*. The Docking results confirmed the obtained results of the antibacterial test showing that the tested compounds are potentially more potent inhibitors than the standard drug Nitroxoline.

#### Declaration of Competing Interest

The authors of this manuscript report that there are no conflicts of interest relevant to this research work.

#### Acknowledgments

The authors recognize the infrastructure and the support of "Ibn Tofaïl, Mohammed V and Umm Al-Qura Universities", and the "National Center for Scientific and Technical Research" for NMR and IR spectra and elemental analysis.

#### Supplementary materials

Supplementary material associated with this article can be found, in the online version, at doi:[10.1016/j.cdc.2020.100593](https://doi.org/10.1016/j.cdc.2020.100593).

#### References

- [1] L.G. Ferreira, A.D. Andricopulo, Drug repositioning approaches to parasitic diseases: a medicinal chemistry perspective, *Drug Discov. Today*. 21 (10) (2016) 1699–1710, doi:[10.1016/j.drudis.2016.06.021](https://doi.org/10.1016/j.drudis.2016.06.021).
- [2] J.P. Oliver, C.A. Gooch, S. Lansing, J. Schueler, J.J. Hurst, L. Sassoubre, M.C. Emily, D.S. Aga, Invited review: fate of antibiotic residues, antibiotic-resistant bacteria, and antibiotic resistance genes in US dairy manure management systems, *J. Dairy Sci.* 103 (2) (2020) 1051–1071, doi:[10.3168/jds.2019-16778](https://doi.org/10.3168/jds.2019-16778).
- [3] G. Vigliotta, D. Giordano, A. Verdino, I. Caputo, S. Martucciello, A. Soriente, A. Marabotti, M. De Rosa, New compounds for a good old class: synthesis of two B-lactam bearing cephalosporins, and their evaluation with a multidisciplinary approach, *Bioorg. Med. Chem.* (28) (2020) 115302, doi:[10.1016/j.bmc.2019.115302](https://doi.org/10.1016/j.bmc.2019.115302).
- [4] K. Mal, B. Naskar, T. Chaudhuri, C. Prodhon, S. Goswami, K. Chaudhuri, C. Mukhopadhyay, Synthesis of quinoline functionalized fluorescent chemosensor for Cu(II), DFT studies, and its application in imaging in living HEK 293 cells, *J. Photochem. Photobiol. A*. 389 (2020) 112211, doi:[10.1016/j.jphotochem.2019.112211](https://doi.org/10.1016/j.jphotochem.2019.112211).
- [5] M.B. Rodrigues, S.C. Feitosa, C.W. Wiethan, W.C. Rosa, C.H. da Silveira, A.B. Pagliari, M.A.P. Martins, N. Zanatta, B.A. Iglesias, H.G. Bonacorso, Ullmann-type copper-catalyzed coupling amination, photophysical, and DNA/HSA-binding properties of new 4-(trifluoromethyl) quinoline derivatives, *J. Fluorine Chem.* 221 (2019) 84–90, doi:[10.1016/j.jfluchem.2019.04.006](https://doi.org/10.1016/j.jfluchem.2019.04.006).
- [6] V. Uppar, K.K. Mudnakudu-Nagaraju, A.I. Basarikatti, M. Chougala, S. Chandrashekarappa, M.K. Mohan, G. Banuprakash, K.N. Venugopala, R. Ninge-gowda, B. Padmashali, Microwave induced synthesis, and pharmacological properties of novel 1-benzoyl-4-bromopyrrolo[1,2-a]quinoline-3-carboxylate analogues, *Chem. Data Collect.* 25 (2020) 100316, doi:[10.1016/j.cdc.2019.100316](https://doi.org/10.1016/j.cdc.2019.100316).
- [7] K.N. Venugopala, V. Uppar, S. Chandrashekarappa, H.H. Abdallah, M. Pillay, P.K. Deb, M.A. Morsy, B.E. Aldhubiab, M. Attimarad, A.B. Nair, N. Sreeharsha, C. Tratratt, A. Yousef Jaber, R. Venugopala, R.P. Mailavaram, B.A. Al-Jaidi, M. Kandeel, M. Haroun, B. Padmashali, Cytotoxicity and antimycobacterial properties of pyrrolo[1,2-a]quinoline derivatives: molecular target identification and molecular docking studies, *Antibiotics* 9 (2020) 1–4, doi:[10.3390/antibiotics9050233](https://doi.org/10.3390/antibiotics9050233).
- [8] V. Uppar, S. Chandrashekarappa, K.N. Venugopala, P.K. Deb, S. Kar, O.I. Alwssil, R.M. Gleiser, D. Garcia, B. Odhav, M.K. Mohan, R. Venugopala, B. Padmashali, Synthesis and characterization of pyrrolo[1,2-a]quinoline derivatives for their larvicidal activity against *Anopheles arabiensis*, *Struct. Chem.* 31 (2020) 1533–1543, doi:[10.1007/s11224-020-01516-w](https://doi.org/10.1007/s11224-020-01516-w).
- [9] D.R. Perez, L.A. Sklar, A. Chigaev, Chloquinol: to harm or heal, *Pharmacol. Ther.* 199 (2019) 155–163, doi:[10.1016/j.pharmthera.2019.03.009](https://doi.org/10.1016/j.pharmthera.2019.03.009).
- [10] E. Meltzer, E. Schwartz, Utility of 8-aminoquinolines in malaria prophylaxis in travelers, *Curr. Infect. Dis. Rep.* 21 (11) (2019) 43, doi:[10.1007/s11908-019-0698-1](https://doi.org/10.1007/s11908-019-0698-1).
- [11] M.E. Mahmoud, M.F. Amira, S.M. Seleim, A.K. Mohamed, Comparative assessment of magnesium-enhanced-extraction by various sequestering derivatives of 8-hydroxyquinoline via layer-by-layer chemical deposition technique, *J. Mol. Liq.* 237 (2017) 455–465, doi:[10.1016/j.molliq.2017.04.096](https://doi.org/10.1016/j.molliq.2017.04.096).
- [12] S.M. Sorouraddin, M.A. Farajzadeh, T. Okhravi, A green solvent less temperature-assisted homogeneous liquid-liquid microextraction method based on 8-hydroxyquinoline simultaneously as complexing agent, and extractant for preconcentration of cobalt, and nickel from water, and fruit juice samples, *Int. J. Environ. An. Ch.* 99 (2) (2019) 124–138, doi:[10.1080/03067319.2019.1578351](https://doi.org/10.1080/03067319.2019.1578351).
- [13] E.J. Velthuisen, B.A. Johns, D.P. Temelkoff, K.W. Brown, S.C. Danehower, The design of 8-hydroxyquinoline tetracyclic lactams as HIV-1 integrase strand transfer inhibitors, *Eur. J. Med. Chem.* 117 (2016) 99–112, doi:[10.1016/j.ejmech.2016.03.038](https://doi.org/10.1016/j.ejmech.2016.03.038).
- [14] M. El Faydy, T. Djassinra, S. Haida, M. Rbaa, K. Ounine, A. Kribii, B. Lakhrissi, Synthesis, and investigation of antibacterial, and antioxidants properties of some new 5-substituted-8-hydroxyquinoline derivatives, *J. Mater. Environ. Sci.* 8 (11) (2017) 3855–3863.

- [15] B. Pippi, W. Lopes, P. Reginatto, F.É.K. Silva, A.R. Joaquim, R.J. Alves, A.M. Fuentefria, New insights into the mechanism of antifungal action of 8-hydroxyquinolines, *Saudi Pharm. J.* 27 (1) (2019) 41–48, doi:[10.1016/j.jsps.2018.07.017](https://doi.org/10.1016/j.jsps.2018.07.017).
- [16] H.R. Zhang, T. Meng, Y.C. Liu, Z.F. Chen, Y.N. Liu, H. Liang, Synthesis, characterization, and biological evaluation of a cobalt (II) complex with 5-chloro-8-hydroxy-quinoline as anticancer agent, *Appl. Organomet. Chem.* 30 (9) (2016) 740–747, doi:[10.1002/aoc.3498](https://doi.org/10.1002/aoc.3498).
- [17] J.O. Odingo, J.V. Early, J. Smith, J. Johnson, M.A. Bailey, M. Files, J. Guzman, J. Ollinger, A. Korkegian, A. Kumar, Y. Ovechkina, Y. Ovechkina, 8-Hydroxyquinolines are bactericidal against *Mycobacterium tuberculosis*, *Drug Dev. Res.* 80 (5) (2019) 566–572, doi:[10.1002/ddr.21531](https://doi.org/10.1002/ddr.21531).
- [18] D. Havrylyuk, B.S. Howerton, L. Nease, S. Parkin, D.K. Heidary, E.C. Glazer, Structure-activity relationships of anticancer ruthenium (II) complexes with substituted hydroxyquinolines, *Eur. J. Med. Chem.* 156 (2018) 790–799, doi:[10.1016/j.ejmech.2018.04.044](https://doi.org/10.1016/j.ejmech.2018.04.044).
- [19] T. Matsui, J. Yamane, N. Mogi, H. Yamaguchi, H. Takemoto, M. Yao, I. Tanaka, Structural reorganization of the bacterial cell-division protein FtsZ from *Staphylococcus aureus*, *Acta Cryst. D.* 68 (2012) 1175–1188, doi:[10.1107/S0907444912022640](https://doi.org/10.1107/S0907444912022640).
- [20] W. Margolin, FtsZ, and the division of prokaryotic cells, and organelles, *Nat. Rev. Mol. Cell Biol.* 6 (11) (2005) 862–871, doi:[10.1038/nrm1745](https://doi.org/10.1038/nrm1745).
- [21] J. Xiao, E.D. Goley, Redefining the roles of the FtsZ-ring in bacterial cytokinesis, *Curr. Opin. Microbiol.* 34 (2016) 90–96, doi:[10.1016/j.mib.2016.08.008](https://doi.org/10.1016/j.mib.2016.08.008).
- [22] J.M. Andreu, C. Schaffner-Barbero, D. Alonso, M.L. Lopez-Rodriguez, L.B. Ruiz-Avila, R. Núñez-Ramírez, O. Llorca, A.J. Martín-Galiano, The antibacterial cell division inhibitor PC190723 is an FtsZ polymer-stabilizing agent that induces filament assembly, and condensation, *J. Biol. Chem.* 285 (2010) 14239–14246, doi:[10.1074/jbc.M109.094722](https://doi.org/10.1074/jbc.M109.094722).
- [23] M. El Faydy, F. Benhiba, H. About, Y. Kerroum, A. Guenbour, B. Lakhri, I. Warad, C. Verma, E.M. Sherif, E.E. Ebnoso, A. Zarruk, Experimental and computational investigations on the anti-corrosive and adsorption behavior of 7-N, N'-dialkylaminomethyl-8-Hydroxyquinolines on C40E steel surface in acidic medium, *J. Colloid Interface Sci.* 576 (2020) 330–344 DOI.org/10.1016/j.jcis.2020.05.010.
- [24] P.C. Taylor, F.D. Schoenkecht, J.C. Sherris, E.C. Linner, Determination of minimum bactericidal concentrations of oxacillin for staphylococcus aureus: influence, and significance of technical factors, *Antimicrob. Agents Chemother.* 23 (1) (1983) 142–150, doi:[10.1128/aac.23.1.142](https://doi.org/10.1128/aac.23.1.142).
- [25] A. Hocquet, M. Langgård, An evaluation of the MM+ force field, *J. Mol. Model.* 4 (1998) 94–112, doi:[10.1007/s008940050128](https://doi.org/10.1007/s008940050128).
- [26] J.J.P. Stewart, Optimization of parameters for semiempirical methods I, *Method. J. Comp. Chem.* 10 (1989) 209–220, doi:[10.1002/jcc.540100208](https://doi.org/10.1002/jcc.540100208).
- [27] K.C. Hsu, Y.F. Chen, S.R. Lin, J.M. Yang, iGEMDOCK: a graphical environment of enhancing GEMDOCK using pharmacological interactions and, post-screening analysis, *BMC Bioinform.* 12 (Suppl. 1) (2011) S33, doi:[10.1186/1471-2105-12-S1-S33](https://doi.org/10.1186/1471-2105-12-S1-S33).
- [28] M. Rbaa, S. Jabli, Y. Lakhri, M. Ouhssine, F.A. Almalki, T. Ben Hadda, S. Messgo-Moumene, A. Zarruk, B. Lakhri, Synthesis, antibacterial properties, and bioinformatics computational analyses of novel 8-hydroxyquinoline derivatives, *Heliyon* 5 (2019) e026892, doi:[10.1016/j.heliyon.2019.e026892](https://doi.org/10.1016/j.heliyon.2019.e026892).
- [29] M. Rbaa, A. Oubih, E.H. Anouar, M. Ouhssine, F.A. Almalki, T. Ben Hadda, A. Zarruk, B. Lakhri, Synthesis of new heterocyclic systems oxazino derivatives of 8-hydroxyquinoline: drug design, and POM analyses of substituent effects on their potential antibacterial properties, *Chem. Data Coll.* 24 (2019) 100306, doi:[10.1016/j.cdc.2019.100306](https://doi.org/10.1016/j.cdc.2019.100306).
- [30] F. Syahira, M. Yusofa, J. Jamalisa, S. Chanderb, R.A. Wahaba, D.P. Bhagwatb, M. Sankaranarayanan, F.A. Almalki, T. Ben Hadda, Psoralen derivatives: recent advances of synthetic strategy, and pharmacological properties, *Antiinflamm. Antiallergy Agents Med. Chem.* (2019), doi:[10.2174/1871523018666190625170802](https://doi.org/10.2174/1871523018666190625170802).
- [31] Z. Sajid, M. Ahmad, S. Aslam, U.A. Ashfaq, A.F. Zahoor, F.A. Saddique, M. Parvez, A. Hameed, S. Sultan, H. Zgou, T. Ben Hadda, Novel armed pyrazolobenzothiazine derivatives: synthesis, X-ray crystal structure, and POM analyses of biological activity against drug resistant clinical isolate of staphylococcus aureus, *Pharm. Chem. J.* 50 (3) (2016) 172–180, doi:[10.1007/s11094-016-1417-y](https://doi.org/10.1007/s11094-016-1417-y).
- [32] J. Sheikh, V. Taile, A. Ghatole, V. Ingle, M. Genc, S. Lahsani, T. Ben Hadda, K. Hatzade, Antimicrobial/antioxidant activity, and POM analyses of novel 7-O- $\beta$ -D-glucopyranosyloxy-3-(4,5-disubstituted imidazol-2-yl)-4H-chromen-4-ones, *Med. Chem. Res.* 24 (6) (2015) 2679–2693, doi:[10.1007/s00044-015-1326-8](https://doi.org/10.1007/s00044-015-1326-8).
- [33] Y.N. Mabkhot, F.D. Aldawsari, S.S. Al-Showiman, A. Barakat, T. Ben Hadda, M.S. Mubarak, S. Naz, Z. Ul-Haq, A. Rauf, Synthesis, bioactivity, molecular docking, and POM analysis of novel substituted thieno[2,3-b]thiophenes, and related congeners, *Molecules* 20 (2015) 1824–1841, doi:[10.3390/molecules20021824](https://doi.org/10.3390/molecules20021824).
- [34] M. Messali, M.R. Aouad, A.A.-S. Ali, N. Rezk, T. Ben Hadda, B. Hammouti, Synthesis, characterization, and POM analysis of novel bioactive imidazolium-based ionic liquids, *Med. Chem. Res.* 24 (2015) 1387–1395, doi:[10.1007/s00044-014-1211-x](https://doi.org/10.1007/s00044-014-1211-x).
- [35] M. Messali, M. Reda Aouad, W.S. El-Sayed, A.A.S. Ali, T. Ben Hadda, B. Hammouti, New eco-friendly 1-alkyl-3-(4-phenoxybutyl) imidazolium-based ionic liquids derivatives: a green ultrasound-assisted synthesis, characterization, antibacterial activity, and POM analyses, *Molecules* 19 (2014) 11741–11759, doi:[10.3390/molecules190811741](https://doi.org/10.3390/molecules190811741).
- [36] H.K. Lautre, S. Das, K. Patil, H. Youssouff, T. Ben Hadda, A.K. Pillai, Evaluation of antimicrobial, and diuretic activity of schiff base metal complexes, part-ii, *World. J. Pharm. Pharm. Sci.* 3 (6) (2014) 1282–1297.
- [37] H.M. Al-Maqtari, J. Jamal, T. Ben Hadda, M. Sankaranarayanan, S. Chander, N.A. Ahmad, H.M. Sirat, I.I. Althagafi, Y.N. Mabkhot, Synthesis, characterization, POM analysis, and antifungal activity of novel heterocyclic chalcone derivatives containing acylated pyrazole, *Res. Chem. Intermed.* 43 (2017) 1893–1907, doi:[10.1007/s11164-016-2737-y](https://doi.org/10.1007/s11164-016-2737-y).
- [38] K.O. Rachedi, R. Bahadi, M. Aissaoui, T. Ben Hadda, B. Belhani, A. Bouzina, M. Berredjem, DFT Study, POM analyses, and molecular docking of novel oxazaphosphinanes: identification of antifungal pharmacophore site, *Indones. J. Chem.* 20 (2) (2020) 440–450, doi:[10.22146/ijc.46375](https://doi.org/10.22146/ijc.46375).
- [39] J.A.I. Rad, A. Jarrahpour, C. Latour, V. Sinou, J.M. Brunel, H. Zgou, Y.N. Mabkhot, T. Ben Hadda, E. Turos, Synthesis, and antimicrobial/antimalarial activities of novel naphthalimido trans- $\beta$ -lactam derivatives, *Med. Chem. Res.* 26 (2017) 2235–2242, doi:[10.1007/s00044-017-1920-z](https://doi.org/10.1007/s00044-017-1920-z).
- [40] G.U. Nasruddin, A. Rauf, H. Khan, N.Z. Mamadialieva, A. Khan, U. Farooq, T. Ben Hadda, M.F. Ramadan, Phytochemical analysis, urease inhibitory effect, and antimicrobial potential of *Allium humile*, *Z. Arz. Gew. Pfl.* 22 (4) (2018) 173–175.
- [41] H. Khan, Z. Khan, S. Amin, Y.N. Mabkhot, M.S. Mubarak, T. Ben Hadda, F. Maione, Plant bioactive molecules bearing glycosides as lead compounds for the treatment of fungal infection: a review, *Biomed. Pharmacother.* 93 (2017) 498–509, doi:[10.1016/j.biopha.2017.06.077](https://doi.org/10.1016/j.biopha.2017.06.077).
- [42] Y.N. Mabkhot, M. Arfan, H. Zgou, Z.K. Genc, M. Genc, A. Rauf, S. Bawazeer, T. Ben Hadda, How to improve antifungal bioactivity: POM, and DFT study of some chiral amides derivatives of Diacetyl-L-tartaric acid, and amines, *Res. Chem. Intermed.* 42 (12) (2016) 8055–8068, doi:[10.1007/s11164-016-2578-8](https://doi.org/10.1007/s11164-016-2578-8).
- [43] Y.N. Mabkhot, A. Alatibi, N. El-sayed, N. Kheder, A. Wadood, A. Rauf, S. Bawazeer, S. Al-Showiman, T. Ben Hadda, Experimental-computational evaluation of antimicrobial activity of some novel armed thiophene derivatives, *Molecules* 21 (2) (2016) 222, doi:[10.3390/molecules21020222](https://doi.org/10.3390/molecules21020222).
- [44] E. Tatar, S. Şenkardeş, H.E. Sellitepe, Ş.G. Küçükgül, Ş.A. Karaoğlu, A. Bozdeveci, E. De Clercq, C. Pannecouque, T. Ben Hadda, I. Küçükgül, Synthesis, prediction of molecular properties, and antimicrobial activity of some acylhydrazones derived from N-(arylsulfonyl)methionine, *Turk. J. Chem.* 40 (3) (2016) 510–534.
- [45] S. Tighadouni, S. Radi, M. Sirajuddin, M. Akkurt, N. Özdemir, M. Ahmad, Y.N. Mabkhot, T. Ben Hadda, In vitro antifungal, anticancer activities, and POM analyses of a novel bioactive schiff base 4-[[[(E)-furan-2-ylmethylidene]amino]phenol: synthesis, characterization, and crystal structure, *J. Chem. Soc. Pak.* 38 (1) (2016) 157–165.
- [46] S. Radi, S. Tighadouni, O. Feron, O. Riant, Y.N. Mabkhot, S.S. Al-Showiman, T. Ben Hadda, M. El-Youbi, R. Benabbes, E. Saalaoui, One pot synthesis, antitumor, antibacterial, and antifungal activities of some Schiff base heterocycles, *Int. J. Pharm.* 5 (1) (2015) 39–45.
- [47] A. Jarrahpour, R. Heiran, V. Sinou, C. Latour, L.D. Bouktab, J.M. Brunel, J. Sheikh, T. Ben Hadda, Synthesis of new  $\beta$ -lactams bearing the biologically important morpholine ring, and POM analyses of their antimicrobial, and antimalarial activities, *Iran. J. Pharm. Res.* 18 (1) (2019) 34–48.
- [48] S. Chander, C.-R. Tang, H.M. Al-Maqtari, J. Jamal, A. Penta, T. Ben Hadda, H.M. Sirat, Y.-T. Zheng, M. Sankaranarayanan, Synthesis, and study of anti-HIV-1 RT activity of 5-benzoyl-4-methyl-1,3,4,5-tetrahydro-2H-1,5-benzodiazepin-2-one derivatives, *Bioorg. Chem.* 72 (2017) 74–79, doi:[10.1016/j.bioorg.2017.03.013](https://doi.org/10.1016/j.bioorg.2017.03.013).
- [49] S. Lahsani, T. Ben Hadda, V. Masand, N.B. Pathan, A. Parvez, I. Warad, U. Shaheen, A. Bader, M. Aljofan, POM analyses of raltegravir derivatives: a new reflection enlighting the mechanism of HIV-integrase inhibition, *Res. Chem. Intermed.* 41 (8) (2015) 5121–5136, doi:[10.1007/s11164-014-1616-7](https://doi.org/10.1007/s11164-014-1616-7).

- [50] K. Bechlem, M. Aissaoui, B. Belhani, K.O. Rachedi, S. Bouacida, R. Bahadi, S.E. Djouad, R.B. Mansour, M. Bouaziz, F.A. Almalki, T. Ben Hadda, M. Berredjem, Synthesis, X-ray crystallographic study, and molecular docking of new  $\alpha$ -sulfamidophosphonates: POM analyses of their cytotoxic activity, *J. Mol. Struct.* 1210 (2020) 127990, doi:[10.1016/j.molstruc.2020.127990](https://doi.org/10.1016/j.molstruc.2020.127990).
- [51] K.T. Rachedi, T.-S. Ouk, R. Bahadi, A. Bouzina, S.-E. Djouad, K. Bechlem, R. Zerrouki, T. Ben Hadda, F.A. Almalki, M. Berredjem, Synthesis, DFT, and POM analyses of cytotoxicity activity of  $\alpha$ -amidophosphonates derivatives: identification of potential antiviral O,O-pharmacophore site, *J. Mol. Struct.* 1197 (2019) 196–203, doi:[10.1016/j.molstruc.2019.07.053](https://doi.org/10.1016/j.molstruc.2019.07.053).
- [52] A. Titi, M. Messali, B.A. Alqurashy, R. Touzani, T. Shiga, H. Oshio, M. Fettouhi, M. Rajabi, F.A. Almalki, T. Ben Hadda, Synthesis, characterization, X-Ray crystal study, and bioactivities of pyrazole derivatives: identification of antitumor, antifungal, and antibacterial pharmacophore sites, *J. Mol. Struct.* 1205 (2020) 127625, doi:[10.1016/j.molstruc.2019.127625](https://doi.org/10.1016/j.molstruc.2019.127625).
- [53] A.M. Kamal, M.I.S. Abdelhady, T. Ben Hadda, Two novel flavone C-glycosides isolated from podocarpus gracilior: POM analyses, and in-vitro anticancer activity against hepatocellular carcinoma, *Int. J. Pharm. Pharm. Sci.* 11 (7) (2019) 57–62, doi:[10.22159/ijpps.2019v11i7.33163](https://doi.org/10.22159/ijpps.2019v11i7.33163).
- [54] F.D. Piaz, A. Bader, N. Malafrente, M. D'Ambola, A.M. Petrone, A. Porta, T. Ben Hadda, N. De Tommasi, A. Bisio, L. Severino, Phytochemistry of compounds isolated from the leaf-surface extract of *Psidia punctulata* (DC.) Vatke growing in Saudi Arabia, *Phytochemistry*. (2018) (IF 2.905) Pub, doi:[10.1016/j.phytochem.2018.08.003](https://doi.org/10.1016/j.phytochem.2018.08.003).
- [55] I. Warad, F.F. Awwadi, M. Daqqa, A.A. Ali, T.S. Ababneh, T.M.A. AlShboul, T.M.A. Jazzazi, F. Al-Rimawi, T. Ben Hadda, Y.N. Mabkhot, New isomeric Cu(NO<sub>2</sub>-phen)2Br complexes: crystal structure, Hirschfeld surface, physicochemical, solvatochromism, thermal, computational, and DNA-binding analysis, *J. Photochem. Photobiol. B*: 171 (2017) 9–19, doi:[10.1016/j.jphotobiol.2017.04.017](https://doi.org/10.1016/j.jphotobiol.2017.04.017).
- [56] M. Genc, Z.K. Genc, S. Tekin, S. Sandal, M. Sirajuddin, .. Ben Hadda, M. Sekerci, Design, synthesis, in vitro antiproliferative activity, binding modeling of 1,2,4-triazoles as new anti-breast cancer agents, *Acta Chimica Slovenica, Acta Chim. Slov.* 63 (4) (2016) 726–737, doi:[10.17344/acsi.2016.2428](https://doi.org/10.17344/acsi.2016.2428).
- [57] M. Genc, Z.K. Genc, S. Tekin, S. Sandal, M. Sirajuddin, T. Ben Hadda, Design, synthesis, in vitro antiproliferative activity, binding modeling of 1,2,4-triazoles as new anti-breast cancer agents", *Acta Chim. Slov.* 63 (4) (2016) 726–737, doi:[10.17344/acsi.2016.2428](https://doi.org/10.17344/acsi.2016.2428).
- [58] A. Rauf, G. Uddin, B.S. Siddiqui, H. Khan, M. ur-Rehman, I. Warad, T. Ben Hadda, S. Patel, A. Khan, U. Farooq, POM analysis of phytotoxic agents from *pistacia integerrima* Stewart, *Curr. Bioact. Compd.* 11 (2015) 231–238, doi:[10.2174/1573407211666151012191902](https://doi.org/10.2174/1573407211666151012191902).
- [59] Y.N. Mabkhot, F. Aldawari, S. Al-Showiman, A. Barakat, S. Soliman, M. Choudhary, S. Yousuf, T. Ben Hadda, M. Mubarak, Synthesis, molecular structure optimization, and cytotoxicity assay of a novel 2-Acetyl-3-amino-5-[(2-oxopropyl)-sulfanyl]-4-cyanothiophene, *Molecules* 21 (2) (2016) 214, doi:[10.3390/molecules21020214](https://doi.org/10.3390/molecules21020214).
- [60] A. Rauf, G. Uddin, B.S. Siddiqui, H. Khan, M. ur-Rehman, I. Warad, T. Ben Hadda, S. Patel, A. Khan, U. Farooq, POM analysis of phytotoxic agents from *pistacia integerrima* Stewart, *Curr. Bioactive Compounds, Curr. Bioact. Compd.* 11 (4) (2015) 231–238, doi:[10.2174/1573407211666151012191902](https://doi.org/10.2174/1573407211666151012191902).
- [61] T. Ben Hadda, Z.K. Genc, V.H. Masand, N. Nebbache, I. Warad, S. Jodeh, M. Genc, Y.N. Mabkhot, A. Barakat, H. Salgado-Zamora, Computational POM, and DFT evaluation of experimental in-vitro cancer inhibition of Staurosporine-Ruthenium(II) complexes: the power force of organometallics in drug design, *Acta Chim. Slov.* 62 (2015) 679–688 <http://dx.doi.org/10.17344/acsi.2015.1357>.
- [62] M.H. Youssoufi, T. Ben Hadda, I. Warad, M.M. Naseer, Y.N. Mabkhot, A. Bader, POM analyses of anti-kinase activity of thirteen peptide alkaloids extracted from *Zizyphus* species, *Med. Chem. Res.* 24 (1) (2015) 267–274, doi:[10.1007/s00044-014-1117-7](https://doi.org/10.1007/s00044-014-1117-7).
- [63] D.Y. Alawadi, H.A. Saadeh, H. Kaur, K. Goyal, R. Sehgal, T. Ben Hadda, N.A. ElSawy, M.S. Mubarak, Metronidazole derivatives as a new class of antiparasitic agents: synthesis, biological activity, and molecular properties prediction, *Med. Chem. Res.* 24 (2015) 1196–1209, doi:[10.1007/s00044-014-1197-4](https://doi.org/10.1007/s00044-014-1197-4).
- [64] V. Amirkhanov, A. Rauf, T. Ben Hadda, V. Ovchinnikov, V. Trush, M. Saleem, M. Raza, T. Rehman, H. Zgou, U. Shaheen, T. Farghaly, Pharmacophores modeling in terms of prediction of theoretical physico-chemical properties, and verification by experimental correlations of carbacylamidophosphates (caph), and sulfanylamidophosphates (saph) tested as new carbonic anhydrase inhibitors, *Mini Rev. Med. Chem.* 19 (12) (2019) 1015–1027, doi:[10.2174/1389557519666190222172757](https://doi.org/10.2174/1389557519666190222172757).
- [65] T. Ben Hadda, O. Talhi, A.S.M. Silva, F.S. Senol, I.E. Orhan, A. Rauf, Y.N. Mabkhot, K. Bachari, I. Warad, T.A. Farghaly, I.I. Althagafi, M.S. Mubarak, Cholinesterase inhibitory activity of some semi-rigid spiro heterocycles: POM analyses, and crystalline structure of pharmacophore site, *Mini Rev. Med. Chem.* 18 (8) (2018) 711–716, doi:[10.2174/1389557517666170713114039](https://doi.org/10.2174/1389557517666170713114039).
- [66] M.A. Ullah, N. Adeel, M.N. Tahir, A. Rauf, M. Akram, T. Ben Hadda, Y.N. Mabkhot, N. Muhammad, F. Naseer, M.S. Mubarak, Synthesis, structural characterization, and antinociceptive activities of new arylated quinolines via Suzuki-Miyaura cross coupling reaction, *Med. Chem.* 13 (8) (2017) 780–786, doi:[10.2174/1573406413666170704100611](https://doi.org/10.2174/1573406413666170704100611).
- [67] Z. Hakkou, A. Maciuc, V. Leblais, N.E. Bouanani, H. Mekhfi, M. Bnouham, M. Aziz, A. Ziyat, A. Rauf, T. Ben Hadda, U. Shaheen, S. Patel, R. Fischmeister, A. Legssyer, Antihypertensive, and vasodilator effects of methanolic extract of *Inula viscosa*: biological evaluation, and POM analysis of cynarin, chlorogenic acid as potential hypertensive, *Biomed. Pharmacother.* 93 (2017) 62–69, doi:[10.1016/j.biopha.2017.06.015](https://doi.org/10.1016/j.biopha.2017.06.015).
- [68] T. Abu-Izneid, A. Maalik, S. Bawazeer, A. Khan, A. Rauf, T. Ben Hadda, H. Khan, M. Fawzy Ramadan, I. Khan, M.S. Mubarak, G. Uddin, A. Bahadar, S.A. Khan, Gastrointestinal mobility, and acute toxicity of pistagremic acid isolated from the galls of *pistacia integerrima*, *Med. Chem.* 13 (3) (2017) 292–294, doi:[10.2174/1573406412666161007145247](https://doi.org/10.2174/1573406412666161007145247).
- [69] A. Rauf, I.E. Orhan, A. Ertas, H. Temel, T. Ben Hadda, M. Saleem, M. Raza, H. Khan, Elucidation of phosphodiesterase-1 inhibitory effect of some selected natural polyphenolics using in vitro, and in silico methods, *Curr. Top Med. Chem.* 17 (4) (2017) 412–441, doi:[10.2174/1568026616666160824103615](https://doi.org/10.2174/1568026616666160824103615).
- [70] E. Header, N. ElSawy, M. El-Boshy, M. Basalamah, M.S. Mubarak, T. Ben Hadda, POM analyses of constituents of *Rosmarinus officinalis*, and their synergistic effect in experimental diabetic rats, *J. Bioanal. Biomed.* 15 (7) (2015) 018–023, doi:[10.4172/1948-593X.1000118](https://doi.org/10.4172/1948-593X.1000118).
- [71] Y.N. Mabkhot, A. Barakat, S. Yousuf, M.I. Choudhary, W. Frey, T. Ben Hadda, M.S. Mubarak, Substituted thieno[2,3-b]thiophenes, and related congeners: synthesis, <math>\beta</math>-glucuronidase inhibition activity, crystal structure, and POM analyses, *Bioorg. Med. Chem.* 22 (23) (2014) 6715–6725, doi:[10.1016/j.bmc.2014.08.014](https://doi.org/10.1016/j.bmc.2014.08.014).
- [72] V. Amirkhanov, A. Rauf, T. Ben Hadda, V. Ovchinnikov, V. Trush, M. Saleem, M. Raza, T. Rehman, H. Zgou, U. Shaheen, T.A. Farghaly, Pharmacophores modeling in terms of prediction of theoretical physico-chemical properties, and verification by experimental correlations of Carbacylamidophosphates (CAPH), and Sulfanylamido-phosphates (SAPH) tested as new carbonic anhydrase inhibitors, *Mini Rev. Med. Chem.* 19 (12) (2019) 1015–1027, doi:[10.2174/1389557519666190222172757](https://doi.org/10.2174/1389557519666190222172757).